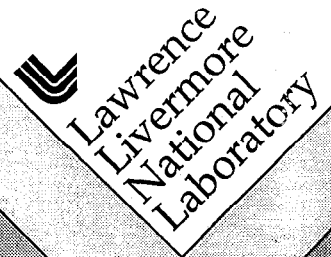


Simulation of Edge-Plasma Profiles and Turbulence Related to L-H Transitions in Tokamaks

T.D. Rognlien
X.Q. Xu
R.H. Cohen

This paper was prepared for submittal to
IAEA Technical Committee Meeting/H-Mode Physics
Oxford, United Kingdom
September 27-29, 1999

September 21, 1999



This is a preprint of a paper intended for publication in a journal or proceedings. Since changes may be made before publication, this preprint is made available with the understanding that it will not be cited or reproduced without the permission of the author.

DISCLAIMER

This document was prepared as an account of work sponsored by an agency of the United States Government. Neither the United States Government nor the University of California nor any of their employees, makes any warranty, express or implied, or assumes any legal liability or responsibility for the accuracy, completeness, or usefulness of any information, apparatus, product, or process disclosed, or represents that its use would not infringe privately owned rights. Reference herein to any specific commercial product, process, or service by trade name, trademark, manufacturer, or otherwise, does not necessarily constitute or imply its endorsement, recommendation, or favoring by the United States Government or the University of California. The views and opinions of authors expressed herein do not necessarily state or reflect those of the United States Government or the University of California, and shall not be used for advertising or product endorsement purposes.

September 21, 1999

Simulation of edge-plasma profiles and turbulence related to L-H transitions in tokamaks

T.D. Rognlien, X.Q. Xu, and R.H. Cohen
Lawrence Livermore National Laboratory
Livermore, CA 94551

Results are presented for fluid transport and turbulence simulations in the edge region of a tokamak using a transport code and a turbulence code. The codes are UEDGE, which calculates two-dimensional plasma and neutral gas profiles, and BOUT, which calculates three-dimensional plasma turbulence using experimental or UEDGE profiles. Both codes describe the plasma behavior using fluid equations.

I. Introduction

Understanding plasma profile evolution and plasma turbulence are two important aspects of developing a predictive model for edge-plasmas in tokamaks and other fusion-related devices. Here we describe results relevant to the L-H transition phenomena observed in tokamaks^{1,2} obtained from two simulations codes which emphasize the two aspects of the problem. UEDGE^{3,4} solves for the two-dimensional (2-D) profiles of a multi-species plasma and neutrals given some anomalous cross-field diffusion coefficients, and BOUT^{5,6} solves for the three-dimensional (3-D) turbulence that gives rise to the anomalous diffusion. These two codes are thus complementary in solving different aspects of the edge-plasma transport problem; ultimately, we want to couple the codes so that UEDGE uses BOUT's turbulent transport results, and BOUT uses UEDGE's plasma profiles with a fully automated iteration procedure. This goal is beyond the present paper; here we show how each aspect of the problem, *i.e.*, profiles and turbulent transport, can contribute to L-H type transitions.

A focus of this paper is the generation of the radial electric field, E_r , in the edge-plasma region. It is known that the shear in the $\mathbf{E} \times \mathbf{B}/B^2$ rotation caused by rapid radial variations in E_r can stabilize plasma instabilities,⁷ and this mechanism is expected to be a major factor in the L-H transition.¹ In our simulations with the UEDGE and BOUT codes, we have a unified treatment of regions on both sides of the magnetic separatrix. There is a natural transition layer about the magnetic separatrix which divides open and closed magnetic field line regions.

The plan of the paper is as follows: In Sec. II, the geometry and basic equations are given. The effects of several parameters the calculated radial electric field from the UEDGE model are presented in Sec. III. Results turbulent diffusion coefficients from the BOUT code are shown in Sec. IV. The conclusions are summarized in Sec. V.

II. Equations and Geometry

The basic models in the UEDGE and BOUT codes are obtained from the plasma fluid equations of continuity, momentum, and thermal energy for both the electrons and ions as given by Braginskii.⁸ In their general three-dimensional form, these six equations represent

ten separate partial differential equations for n_e , n_i , \mathbf{v}_e , \mathbf{v}_i , T_e , and T_i . UEDGE and BOUT use similar assumptions to reduce the complexity of their models. Both codes solve for the variables n_i , $v_{i\parallel}$, T_e , T_i , and the electrostatic potential, ϕ . The current continuity equation is used as the equation for ϕ . In addition, BOUT solves for the magnetic vector potential, A_{\parallel} . Both codes assume that the perpendicular ion motion is dominated by the $\mathbf{E} \times \mathbf{B}$ and diamagnetic velocities, with corrections from the ion viscosity tensor; BOUT also includes the full inertial terms as important corrections for the turbulence. More details of these models can be found in Refs. 3–5,11.

Both UEDGE and BOUT use the same mesh in the poloidal plane based on poloidal magnetic flux surfaces from an MHD equilibrium code such as EFIT, with an orthogonal, or sometimes non-orthogonal, flux-surface-aligned. Typically a region several centimeters inside and outside the magnetic separatrix is included. Both codes use fully implicit Newton-Krylov to advance the finite-differenced equations in time or to find steady-state equilibrium profiles (for UEDGE).¹²

III. Equilibrium edge-plasmas using UEDGE

The shear in the radial electric field, E_r , is believed important to the stabilization of edge turbulence which allows the discharge to make the transition to H-mode confinement with an edge transport barrier.¹ We consider the variation of E_r obtained from the UEDGE equilibrium model with three quantities: core power, perpendicular ion viscosity, and charge uncovering due to possible prompt ion loss near the separatrix. Variations are performed about a base-case for the single-null DIII-D tokamak geometry⁹ using a core-edge density of $3 \times 10^{19} \text{ m}^{-3}$, and a total power of 2 MW split equally between ions and electrons. The ion ∇B drift is toward the X-point, and the plate recycling coefficient is varied from $R_p = 0.95$. Constant turbulent radial diffusion coefficients of $0.5 \text{ m}^2/\text{s}$ are used, except that the ion perpendicular viscosity is allowed to vary in one subsection.

Experimentally, it is observed that the L-H mode transition occurs as the auxiliary heating to the plasma core increases.¹ We model that here with a series of UEDGE calculations where the ion and electron core power is varied. The resulting E_r radial profile at the outer midplane is shown in Fig. 1. The depth of the well in E_r is a strong function of total power,

split evenly between ions and electrons. The $\mathbf{E} \times \mathbf{B}$ velocity varies as E_r/B and thus has a strong shear where E_r does. There is therefore a natural evolution to a stronger shear layer as the power is increased, favoring suppression of turbulence. In an earlier paper,⁴ we showed how a reduction of all the turbulent diffusion coefficients likewise leads to a deepening of the E_r well. Thus, these two effects can work together to cause a rapid suppression of turbulence, although a full dynamical model remains to be done. In part, the deeper E_r -well is caused by the larger ion pressure gradient at higher power, but the total effect is stronger than one would expect based on ion pressure balance alone.

In the UEDGE model, the radial current component in the current continuity equation that depends on ϕ explicitly is modeled as arising from a (turbulently) enhanced ion perpendicular viscosity.^{4,10} This current is given by

$$J_{r,v} = \frac{q}{\omega_{ci}} \frac{\partial}{\partial r} n \nu_{a\perp} \frac{\partial}{\partial r} V_g \quad (1)$$

where $\nu_{a\perp}$ is the viscosity coefficient, and $V_g = [-E_r + \nabla_r P_i / (qn)] / B$ is the ion perpendicular drift velocity lying in the flux surface. For a turbulence-enhanced value of $\nu_{a\perp} \sim 0.5 \text{ m}^2/\text{s}$, the magnitude of this current is still typically small compared to the ∇B current, yet it yields the needed dependence on ϕ to allow one to solve for the potential in moving across the separatrix from the open to closed B-field line region. The dependence of the E_r profile on the magnitude of $\nu_{a\perp}$ is shown in Fig. 2. Over the order-of-magnitude range shown, the viscous current plays the role of connecting the solutions determined by the different open and closed field-line physics, and its the magnitude is not very important. There is still an issue of whether or not a diffusive description of this turbulence-driven current is appropriate, and in Sec. IV, we use BOUT to measure an effective $\nu_{a\perp}$.

Finally, we estimate the influence of a prompt loss of core ions near the separatrix edge.¹⁴ These losses can occur for sufficiently hot edge ions whose banana orbits contact boundary surfaces. This is simply modeled as a uniform ion particle sink in the outer-half of the core-edge region; in practice, this region should be limited to about one poloidal gyroradius ($\sim 1 - 2 \text{ cm}$ in DIII-D). The current continuity equation thus becomes

$$\nabla \cdot \mathbf{J} = -I_{pl} H_{oc} / V_{oc} \quad (2)$$

where H_{oc} is unity in the outer 1/2 of the core-edge region and zero elsewhere, and V_{oc} is the volume of the outer core-edge region. The current I_{pl} gives the total magnitude of

the assumed prompt-loss current. The same sink term, divided by q , appears in the ion continuity equation.

The effect of this charge imbalance is mitigated some by the parallel electron (Pfirsch-Schluter) currents, and the net effect can be determined from our model. The results of three cases with $I_{pl} = 0, 250$, and 500 A are shown in Fig. 3. The qualitative change is to further decrease E_r which can be deduced from Eqs. (1) and (2): a large v''' and thus, in the shear layer, a more negative E_r , is required to satisfy current continuity and so maintain quasineutrality. Determining the magnitude of the change requires the more complete UEDGE model. Figure 3 implies that a prompt-loss current of more than 250 Amps is required to have much effect for our DIII-D case. Note also that the response is nonlinear, with the incremental decrease in E_r from 500 Amps being much more than twice the 250 Amp case.

IV. Turbulent diffusion coefficients from BOUT

As discussed in Sec. III, the UEDGE code uses enhanced classical ion perpendicular viscosity $\nu_{a\perp}$ to model the radial current as described in Eq. (1). In this section we give a derivation of an equivalent turbulent viscosity which we still term $\nu_{a\perp}$, and use BOUT to measure it.

Starting from the momentum equations and using the well-known gyro-viscous cancellation, the total momentum equation becomes

$$nm_i \frac{\partial \mathbf{V}}{\partial t} + nm_i (\mathbf{V}_E + V_{\parallel i} \mathbf{b}_0) \cdot \nabla \mathbf{V} = -\nabla \left[P_i + P_e + \frac{P_i}{2\omega_{ci}} \nabla_{\perp} \cdot (\mathbf{b} \times \mathbf{V}) \right] + \frac{1}{c} \mathbf{J} \times \mathbf{B}. \quad (3)$$

Equation (3) can be combined with the continuity equation to yield the momentum density equation. The $\nabla \psi \times \mathbf{b}_0/B$, or geodesic, component of the momentum equation yields an expression for the radial current. Averaging this current over a toroidal angle and over the fluctuation time scale yields

$$\mathcal{J} \cdot \nabla \psi = \frac{1}{J_{ac}} \frac{\partial}{\partial \psi} \left(\Gamma_{\perp} |\nabla \psi|^2 J_{ac} \right), \quad (4)$$

$$\Gamma_{\perp} = m_i c \frac{\langle n R V_g (\mathbf{V}_E + V_{\parallel i} \mathbf{b}) \cdot \nabla \psi \rangle}{|\nabla \psi|^2}, \quad (5)$$

$$R V_g \simeq -\frac{c |\nabla \psi|^2}{B^2} \left(\frac{\partial \phi}{\partial \psi} + \frac{1}{n q} \frac{\partial P_i}{\partial \psi} \right). \quad (6)$$

Where we have used the definition of the magnetic field $\mathbf{B} = I(\psi)\nabla\varphi + \nabla\varphi \times \nabla\psi$, with ψ being the poloidal magnetic flux and φ being the toroidal angle. Also, J_{ac} is Jacobian, R is the major radius, and Γ_{\perp} is the turbulence-generated geodesic momentum flux. The key ballooning assumption is $d/d\theta \simeq -q\partial/\partial\varphi$ for annihilation of the additional poloidal derivative terms for the fluctuations. Assuming the geodesic momentum flux is diffusive, as is done in the UEDGE simulations, and as may be expected when the momentum convection is small, the turbulence-generated viscous momentum flux can then be written as

$$\Gamma_{\perp} = -\nu_{a\perp} \frac{\partial}{\partial\psi} (nm_i R V_g). \quad (7)$$

This equation is used to calculate $\nu_{a\perp}$ using Γ_{\perp} measured from BOUT and $nm_i V_g$ from the equilibrium profiles. A similar turbulent viscous momentum flux has been given by Hinton and Kim¹⁵ from a kinetic theory and from the fluid turbulence theory.¹⁶ The turbulent viscosity $\nu_{a\perp}$ plays a role similar to the classical perpendicular ion viscosity ν_{ii} , generating the radial current in order to satisfy the quasi-neutrality in boundary plasmas across the magnetic separatrix.

The measured turbulent viscosity $\nu_{a\perp}$ from the BOUT simulation is shown in Fig. 4 (solid line). The magnitude of this viscosity is typically similar to the particle and heat diffusivities, such as the ion heat diffusivity χ_i shown in Fig. 4 (dashed line). However, note that the viscosity is not always positive, indicating there exists non-diffusive transport of the perpendicular momentum. BOUT typically calculates the turbulent self-generated electric field. In the measurement of turbulent viscosity shown in Fig. 4, this field is set to zero. When the turbulent self-generated electric field calculation is turned on, the turbulent viscosity is even more negative due to the non-zero turbulent convection. The turbulent viscous momentum flux has strong poloidal dependence and has opposite signs in different poloidal locations. Therefore the radial current also has opposite signs in different poloidal locations, and it does not charge the plasma due to the global charge conservation. In contrast, the heat fluxes are positive along the flux surface, and the heat flows out from the core to the scrape-off layer across the magnetic separatrix as expected. The constraint for global ambipolarity $\oint \mathbf{ds} \cdot \mathbf{J} \simeq 0$ on the last closed flux is numerically satisfied in BOUT by using the radial current given by Eq. (4). The radial current J_{ψ} flows out at the midplane and flows in near the X-point regions. The parallel current in the SOL flows to the X-point regions and connects them to close the loop.

V. Conclusions

We have presented simulation results from the 2-D UEDGE transport code and the 3-D BOUT turbulence code to elucidate various physical mechanism relevant to the L-H transition regime for edge plasmas. The variation of the radial electric field, E_r , with the following parameters has been investigated with UEDGE: power from the core plasma, anomalous perpendicular viscosity coefficient, and charge uncovering from prompt ion losses. With the exception of the magnitude of the perpendicular viscosity coefficient, these effects can have a strong effect on the depth of the E_r well, and its radial gradient. The resulting shear in the E_r/B poloidal velocity can substantially reduce the turbulence transport in the edge-plasma region as shown by detailed BOUT simulations for DIII-D parameters reported elsewhere.¹¹

We have also performed BOUT simulations which begin with initial experimental profiles from DIII-D, but then evolve the background profiles of ion temperature and density by using sources near the core boundary and sinks in the scrape-off layer region. For sufficient ion heating (similar to the experiment), this model shows a transition from L-mode-like state with high turbulent edge transport to H-mode-like state with much reduced transport. The details on these simulations are discussed elsewhere.¹⁷

Acknowledgments: Work performed under the auspices of the USDOE by the Lawrence Livermore National Laboratory under contract number W-7405-ENG-48. It is a pleasure to thank D.D. Ryutov for many helpful discussions.

References

- ¹K.H. Burrell, Phys. Plasmas **4**, 1499 (1997).
- ²K. Ida, Plasma Phys. Contr. Fusion **40**, 1429 (1998).
- ³T.D. Rognlien, P.N. Brown, R.B. Campbell, *et al.*, Contrib. Plasma Phys. **34**, 362 (1994).
- ⁴T.D. Rognlien, D.D. Ryutov, N. Mattor, and G.D. Porter, Phys. Plasmas **6**, 1851 (1999).
- ⁵Xueqiao Xu and Ronald H. Cohen, Contrib. Plasma Phys. **38**, 158 (1998).
- ⁶X.Q. Xu, R.H. Cohen, G.D. Porter, *et al.*, J. Nucl. Mater. **266-269**, 654 (1999).
- ⁷H. Biglari, P.H. Diamond, and P.W. Terry, Phys. Fluids B **2**, 1 (1990).
- ⁸S.I. Braginskii, "Transport Processes in a Plasma", in *Reviews of Plasma Physics*, Vol. I, Ed. M.A. Leontovich (Consultants Bureau, New York, 1965), p. 205.
- ⁹J.L. Luxon, P. Anderson, F. Batty, *et al.*, in Proc. 11th Int. Conf. Plasma Phys. Controlled Nucl. Fusion (IAEA, Vienna, 1987), p. 159.
- ¹⁰T.D. Rognlien, G.D. Porter, and D.D. Ryutov, J. Nucl. Mater. **266-269**, 654 (1999).
- ¹¹X.Q. Xu, R.H. Cohen, G.D. Porter, *et al.*, Nucl. Fusion, to be published (1999).
- ¹²P.N. Brown and A.C. Hindmarsh, J. Appl. Math. Comp. **31**, 40 (1989).
- ¹³A.V. Chankin, J. Nucl. Mater. **241-243**, 199 (1997).
- ¹⁴K. C. Shaing, and E. C. Crume Jr, Phys. Rev. Lett. **63**, 2369 (1989).
- ¹⁵F. L. Hinton, Y. -B. Kim, Nuclear Fusion **34**, 899(1994).
- ¹⁶N. Mattor, private communication.
- ¹⁷X.Q. Xu, invited paper, APS-DPP Conference, Seattle, WA, Nov. 15-19, 1999; to be published in Phys. Plasmas.

Figures

FIG. 1. The radial electric field, E_r , at the outer midplane versus position from the magnetic separatrix for four levels of power crossing the core boundary.

FIG. 2. Radial profiles of E_r for several values of $\nu_{a\perp}$, the perpendicular ion viscosity in Eq. (1).

FIG. 3. Radial profiles of E_r for several values of the prompt-loss ion current, I_{pl} , in Eq. (2).

FIG. 4. The turbulent diffusion coefficients from BOUT: (a), the perpendicular turbulent viscosity $\nu_{a\perp}$; and (b), the ion heat diffusivity χ_i .

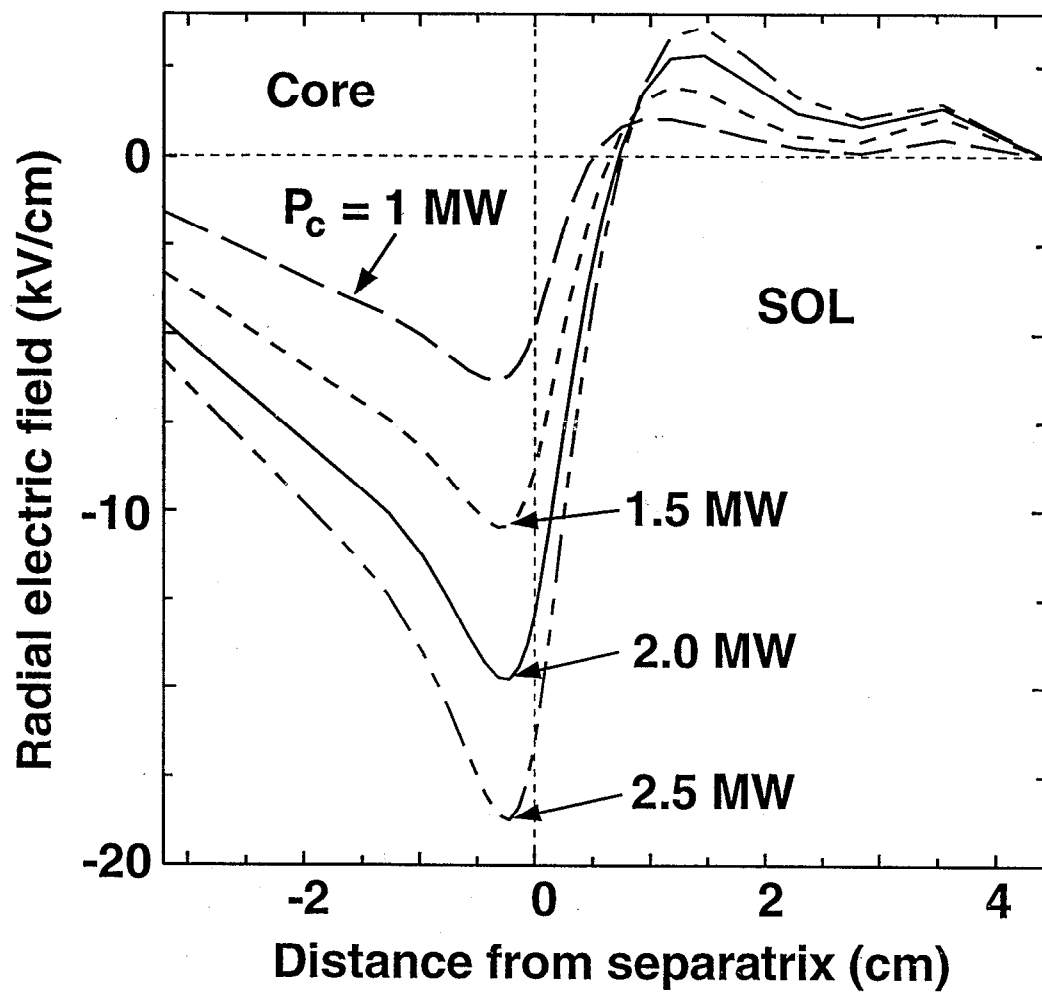


Fig. 1

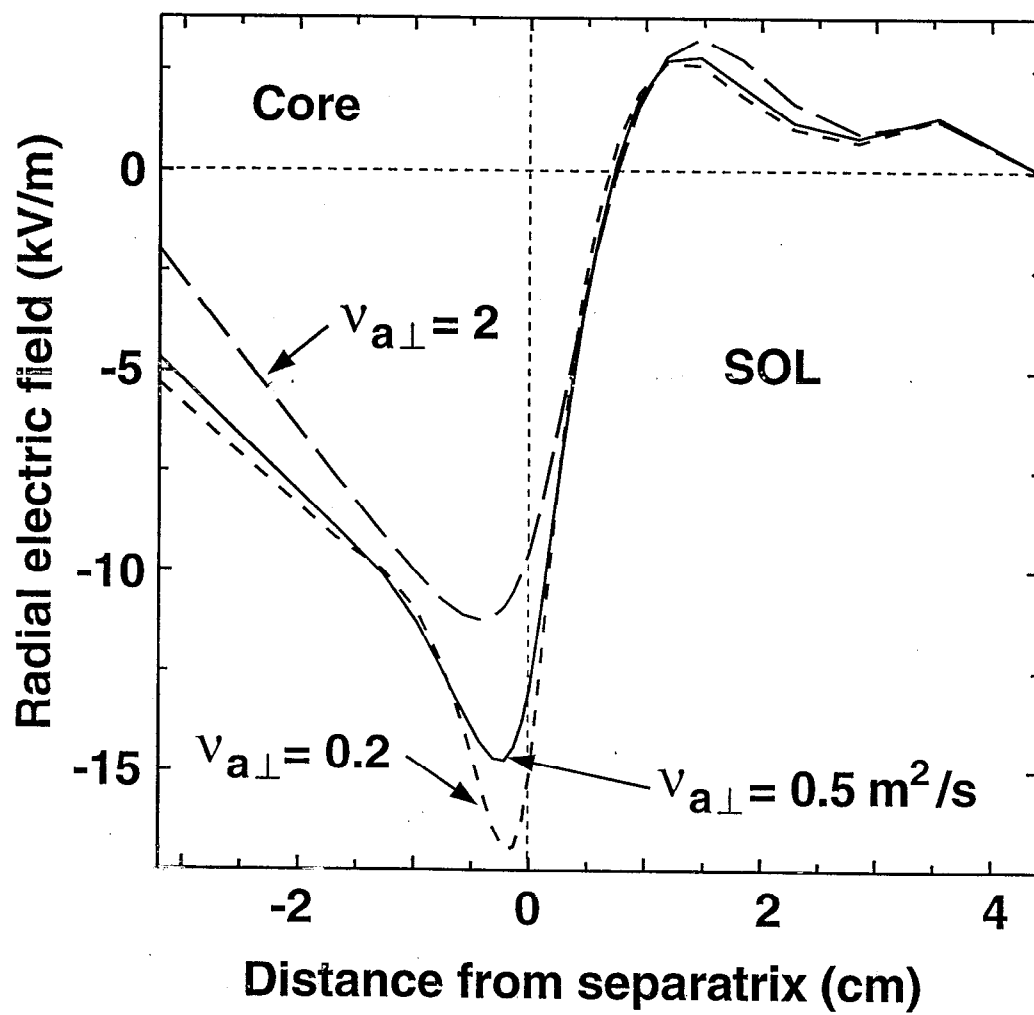


Fig. 2

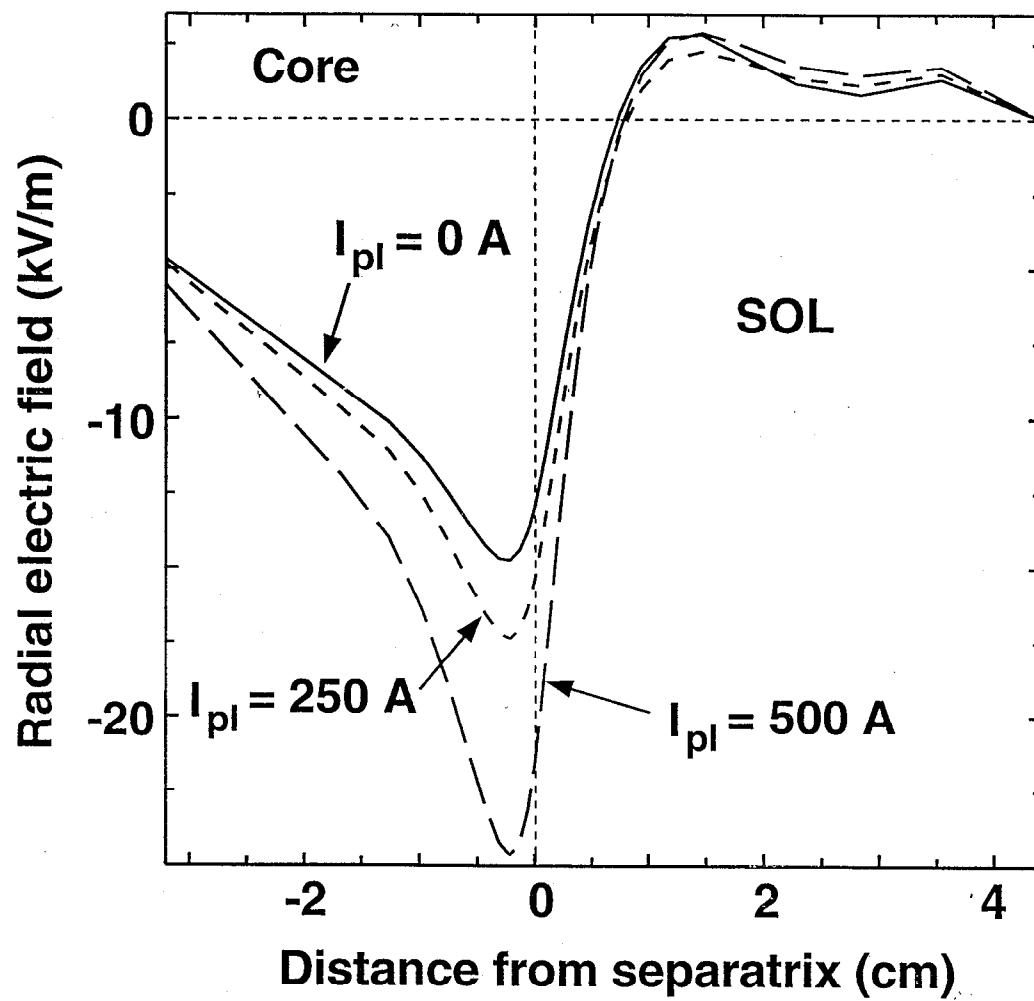


Fig. 3

